



## Influence of pH and calcination temperature on the properties of synthesized ceria

Sarath Menon, Shiv Kumar Manu, S. Noyel Victoria and R. Manivannan\*

Department of Chemical Engineering, National Institute of Technology Raipur, Raipur-492 010, Chhattisgarh, India

E-mail: rmani.che@nitrr.ac.in

Manuscript received online 20 April 2020, accepted 01 June 2020

Ceria particles are now extensively used in chemical mechanical polishing of glass, which makes them a promising material for semiconductor industry. In this work, a facile co-precipitation route was adopted to synthesis ceria particles. Cerium nitrate hexahydrate and sodium carbonate were used as the precursors. Study of the effect of pH and calcination temperature on synthesized ceria particles were carried out in detail. The surface morphology was found to be influenced significantly by change in solution pH, as evinced from SEM results. XRD spectra revealed improvement in crystallite size for synthesized nanoceria calcined at different temperatures.

Keywords: Nanoparticles, ceria, pH, calcination temperature.

### Introduction

Ceria is a rare earth material having face centered cubic fluorite structure<sup>1</sup>. In recent years' ceria as a nanoparticle have gained wide attentiveness in research domain. Because, unlike their bulk counterparts, they possess captivating immanent physical and chemical properties<sup>2</sup>. Immense potential uses of ceria have been observed as an outcome of burgeoning academic interest on them. Some salient applications being: as an electrolyte material for solid oxide fuel cells (SOFC), as sunscreen for ultraviolet absorbents, in oxygen sensors, as ceramic pigments, as catalytic wet oxidation material and for photocatalytic oxidation of water<sup>3</sup>. Currently both industrial and academic focus on ceria nanoparticles are deeply rooted to their use as an abrasive in silicon substrate chemical mechanical polishing (CMP) and modern automotive engine exhaust catalyst<sup>4</sup>.

Prescience behind the promising nature of nanoceria and nanoceria based compounds, with different properties for different applications, emerged with a large number of conventional and novel methods for its synthesis. These methods include precipitation, hydrothermal, sono-chemical, solution combustion, ultra-sonic spray pyrolysis and hydroxide mediated approach<sup>5</sup>. Selection of proper techniques depends on both the required specific properties and accessibility of reagent chemicals<sup>6</sup>. Among these methods, owing to its

comparably simpler, inexpensive nature and easy scale-up, precipitation method has gained ample attention<sup>7</sup>. Chen *et al.* synthesized nanoceria by precipitation using cerium nitrate and ammonia as precursors to evaluate the effect of reaction temperature and atmosphere on its characteristics<sup>8</sup>. Liu *et al.* prepared nanoceria particles about 200 nm size with cerium sulphate and oxalic acid as precursors<sup>9</sup>. Cerium nitrate, potassium carbonate and potassium hydroxide were used as precursors by Farahmandjou *et al.* to synthesis cerium oxide nanoparticles via co-precipitation route<sup>5</sup>. Cerium precursors in nitrate form are reported to be most preferred for producing nanoceria particles with uniform size<sup>10</sup>. Most literatures on precipitation technique were evolving around influence of cerium precursors, additives, reaction atmosphere and ligands<sup>7</sup>. Whilst very few reported works are available on effects of pH and calcination temperature. In this paper, a facile co-precipitation method to synthesize cerium oxide nanoparticles is reported. Further the influence of pH on morphology and calcination temperature on crystallite growth of prepared particles was investigated with the aid of SEM, EDS and XRD.

### Experimental

Cerium nitrate hexahydrate ( $\text{Ce}(\text{NO}_3)_3 \cdot 6\text{H}_2\text{O}$ : 99.9%) and sodium carbonate ( $\text{Na}_2\text{CO}_3$ : anhydrous 99.5%: extra pure) were purchased from Loba Chemie.

Requisite amount of cerium nitrate and sodium carbonate precursors were weighed precisely and dissolved in 250 mL of water. Then the freshly prepared 0.1 M cerium nitrate and 0.15 M sodium carbonate aqueous solutions were added drop by drop to 100 mL of well stirred distilled water simultaneously in required quantity. Precipitation of cerous carbonate occurs immediately and much more progressively. Thereupon, the solution was parted to three. NaOH/nitric acid was added to adjust the pH of solutions to acidic (5), neutral (7) and alkaline (9). Solutions were then dried for 2 h at 80°C in a hot air oven and brought to room temperature. Without any purification, solutions were aged in a muffle furnace for 2.5 h at 230°C. Finally, the sample was calcined at 600°C for 3 h to produce ceria nanoparticles. XRD analysis of the sample was carried out with  $2\theta$  in range 20–90° (scan rate: 3.5°/min) using PANalytical 3Kw Xpert Powder XRD to identify crystalline size and phase. The morphology of prepared nanoceria was characterised by SEM with type ZEISS EVO-18. Elemental composition was studied using EDS (INCA 250 EDS).

## Results and discussion

### *Influence of pH:*

Fig. 1 evinces the SEM images of ceria particles synthesized at different pH values. The significant effect of solute environment in defining the surface morphology of grains was reported in most of the existing literatures<sup>11</sup>. At acidic condition (Fig. 1a), softly agglomerated small crystallites were observed. Ceria nanoparticle tends to aggregate and evolve

into an irregular complex mixture of spherical and rod like assembly at neutral environment<sup>12</sup> (Fig. 1b). Clearly defined cubical flake like morphology of nanoceria aggregates (Fig. 1c) were found in alkaline pH. This can be attributed to the effect of nucleation of nanoparticles. Elemental composition of nanoceria synthesized at different pH was affirmed by EDS results as reported in Table 1.

**Table 1.** Elemental composition of prepared nanoceria at different pH

Element	Weight (%)		
	Acidic	Neutral	Basic
O	15.32	23.17	16.50
K	–	0.88	1.35
Ce	84.68	75.95	82.15

Fig. 2 revealed the XRD morphology of nanoceria particles prepared at different pH conditions. Spectra peaks at 28.5°, 33.1°, 47°, 56.3°, 69.5°, 76.7° and 79.1° corresponds to (111), (200), (220), (311), (222), (400), (331), (420) and (422) respectively of cerium oxide with fluorite cubic structure. Crystallite diameter and average crystallite size is reported in Table 2. A decline in average crystallite size with rise in pH of solute environment was observed. This is in congruence with existing literatures<sup>11,13</sup>.

### *Effect of calcination:*

XRD patterns of synthesized ceria nanoparticles at different calcination temperatures evidenced the pure crystal-

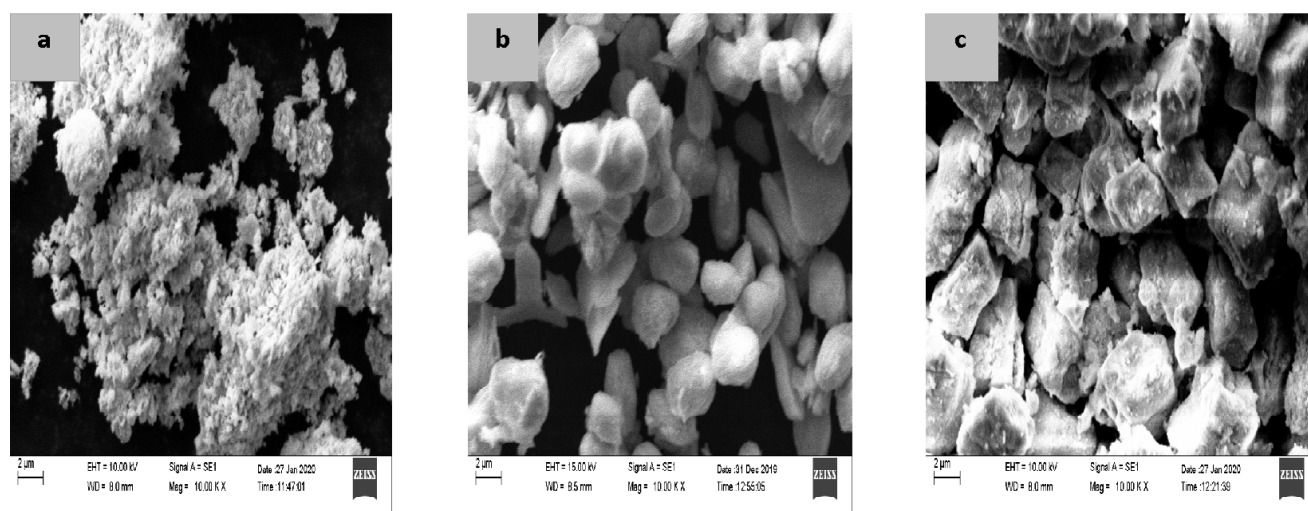


**Fig. 1.** SEM images of nanoceria synthesized at (a) acidic, (b) neutral and (c) alkaline condition.

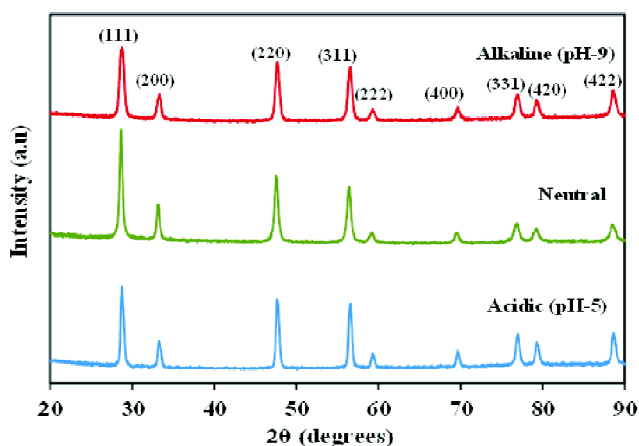


Fig. 2. XRD patterns of synthesized nanoceria at different pH.

Table 2. Characterization data on influence of pH

Sample	XRD	
	Crystallite diameter ( <i>D</i> ) (nm)	Average crystallite size (nm)
Acidic	16	17
Neutral	18	14
Alkaline	11	13

line nature of as-synthesized particles as shown in Fig. 3. Each sample evinces distinctive peaks corresponding to (111), (200), (220), (311) planes which closely confirms to fluorite structured CeO<sub>2</sub> crystal. Prior to calcination, broad XRD peaks were observed at (111), (200), (220) and (311).

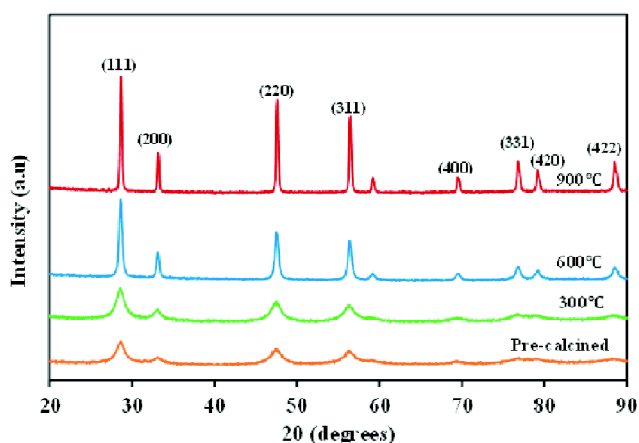


Fig. 3. XRD patterns of synthesized nanoceria at various calcination temperatures.

On increasing the temperature, peaks become sharper along with an addition of five more peaks at (222), (400), (331), (420) and (422). This gives a plausible reason for the rise in crystallization. According to Debye-Scherrer equation<sup>10</sup>:

$$D = \frac{0.89 \lambda}{B \cos \theta} \quad (1)$$

crystallite size of the synthesized ceria particles at each calcination temperature has been estimated. Table 3 summarizes the crystallite diameter and average crystallite size corresponding to calcination temperature. In general, crystallite size is deliberated using the strong peak, while the average crystallite size is deliberated using all the peaks obtained in the XRD spectra<sup>13</sup>. With the increase in calcination temperature, a proliferating trend can be observed in both the results. Small crystallite sizes prior to and at low calcination temperatures can be attributed to high porosity and interconnection between the pores<sup>14</sup>. Network of continuous particle boundaries have been able to be formed at higher temperatures by linking of fine particles, thus improving the size of crystals<sup>10</sup>.

Table 3. Characterisation data on effect of calcination temperature

Sample	XRD	
	Crystallite diameter ( <i>D</i> ) (nm)	Average crystallite size (nm)
Pre-calcined	6	5
Calcined at 300°C	7	6
Calcined at 600°C	18	15
Calcined at 900°C	29	25

### Conclusions

Ceria particles were synthesised successfully by adopting a facile co-precipitation route using cerium nitrate and sodium carbonate as precursors. XRD results ascertained the cubic fluorite structure of prepared nanoceria. Influence of pH on surface morphology of ceria nanoparticles was evident from SEM images with significant changes in each case. Irregular, small and agglomerated crystals were observed in acidic conditions. Neutral environment resulted in complex mixture of spherical and rod like assembly, while in alkaline state defined cubical morphology was obtained. Also, average crystallite size tends to decrease from acidic to alkaline

conditions. On increasing, calcination temperature strongly affirms its significance on crystallite size. Small crystals at lower temperature attain improvement in crystallinity at higher temperature.

#### References

1. M. Jalilpour and M. Fathalilou, *Int. J. Phys. Sci.*, 2012, **7**, 944.
2. N. K. Renuka, *J. Alloys Compd.*, 2012, **513**, 230.
3. A. I. Y Tok, L. H. Luo, F. Y. C Boey and J. L. Woodhead, *J. Mater. Res.*, 2006, **21**, 119.
4. T. S. Sreeremya, M. Prabhakaran and S. Gosh, *RSC Adv.*, 2015, **5**, 84056.
5. M. Farahmandjou, M. Zarinkamar and T. P. Firoozabadi, *Rev. Mex. Fis.*, 2016, **62**, 496.
6. S. Sciré and L. Palmisano, *Metal Oxides*, 2020, 1.
7. J. C. Chen, W. C. Chen, Y. C. Tien and C. J. Shih, *J. Alloys Compd.*, 2010, **496**, 364.
8. H. I. Chen and H. Y. Cheng, *Solid State Commun.*, 2004, **133**, 593.
9. Y. H. Liu, J. C. Zuo, X. F. Ren and L. Yong, *METALURGIJA*, 2014, **53**, 463.
10. K. K. Babitha, A. Sreedeevi, K. P. Priyanka, B. Sabu and T. Varghese, *Indian J. Pure Appl. Phys.*, 2015, **53**, 596.
11. M. Ramachandran, R. Subadevi and M. Sivakumar, *Vaccum*, 2019, **161**, 220.
12. M. Yan, W. Wei and N. Zouren, *J. Rare Earth*, 2007, **25**, 53.
13. A. S. Saleemi, A. Abdullah and M. A. Rehman, *J. Supercond. Nov. Mag.*, 2013, **26**, 1065.
14. T. Lai, Y. Shu, G. Huang, C. Lee and C. Wang, *J. Alloys Compd.*, 2008, **450**, 318.